Balanced Ocean-Data Assimilation near the Equator

GERRIT BURGERS

Royal Netherlands Meteorological Institute, De Bilt, Netherlands

MAGDALENA A. BALMASEDA

European Centre for Medium-Range Weather Forecasts, Reading, Berkshire, United Kingdom

FEMKE C. VOSSEPOEL

Laboratoire d'Océanographie Dynamique et de Climatologie, Paris, France

GEERT JAN VAN OLDENBORGH

Royal Netherlands Meteorological Institute, De Bilt, Netherlands

PETER JAN VAN LEEUWEN

Institute for Marine and Atmospheric Research Utrecht, Utrecht University, Utrecht, Netherlands

(Manuscript received 18 July 2001, in final form 3 January 2002)

ABSTRACT

The question is addressed whether using unbalanced updates in ocean-data assimilation schemes for seasonal forecasting systems can result in a relatively poor simulation of zonal currents. An assimilation scheme, where temperature observations are used for updating only the density field, is compared to a scheme where updates of density field and zonal velocities are related by geostrophic balance. This is done for an equatorial linear shallow-water model. It is found that equatorial zonal velocities can be detoriated if velocity is not updated in the assimilation procedure. Adding balanced updates to the zonal velocity is shown to be a simple remedy for the shallow-water model. Next, optimal interpolation (OI) schemes with balanced updates of the zonal velocity are implemented in two ocean general circulation models. First tests indicate a beneficial impact on equatorial upper-ocean zonal currents.

1. Introduction

For seasonal forecasts with coupled general circulation models, a good analysis of the upper equatorial oceans is essential. Ocean-data assimilation has contributed significantly to the success of operational systems (Stockdale et al. 1998; Ji et al. 1996). These systems use optimal interpolation (OI) schemes and three dimensional variational (3D-VAR) schemes that assimilate in situ subsurface temperature observations for updating the 3D temperature field (Smith et al. 1991; Behringer et al. 1998; Segschneider et al. 2000; Alves et al. 2001). Extended schemes are being developed and tested that in addition assimilate sea-level anomalies observed by satellite radar altimeters. These extended schemes also update the 3D temperature field (Ji et al. 2000) and sometimes the 3D salinity field as well (Vossepoel and Behringer 2000; Segschneider et al. 2000; Alves et al. 2001).

In all these applications, observations are used for updating variables that change the density field, not the velocity field. This is in marked contrast to the situation in meteorology, where initialization is a delicate problem and updates of the density field and the velocity field have to be related. Various methods exist, see, for example, the textbook of Daley (1991). One of the more direct, and simple, is OI with covariances that enforce a geostrophic balance of velocity and height increments. Oceanographers are well aware of this, and also in oceanography often balances are exploited in data assimilation. Examples are Oschlies and Willebrand (1996), who related sea-surface height increments from altimeter measurements through velocity increments to density increments in a primitive equation model of the North Atlantic, and Ishikawa et

Corresponding author address: Gerrit Burgers, Oceanographic Research Division, Royal Netherlands Meteorological Institute (KNMI), P.O. Box 201, 3730 AE De Bilt, Netherlands.
E-mail: burgers@knmi.nl

al. (2001), who constructed a 3-D VAR assimilation scheme for a 1.5-layer model of the western part of the North Pacific. Bell et al. (2001) propose a scheme for making balanced corrections to compensate the bias in an ocean model near the equator. In some advanced types of assimilation schemes, the appropriate balance is automatically ensured. This is, for instance, the case for a Kalman filter, if both velocities and densities are updated, and in 4D-VAR, if the driving fluxes of the ocean are the control variables, as in the study of Bonekamp et al. (2001).

However, the question of balance usually is ignored in optimal interpolation schemes for equatorial ocean models that simulate interannual variability. For this, there are two main reasons. The first is that, the larger the scale, the more the height field and the less the velocity field dominates the potential vorticity and determines the adjustment (Daley 1991). Although much larger than the Rossby radius in mid latitudes, the typical baroclinic equatorial Rossby radius is only of the order of 300 km, which is small compared to the zonal scale of ENSO variability. Consequently, not paying attention to velocities is relatively harmless. The second reason is that the very simplest form of balance, geostrophic balance, breaks down at the equator where the Coriolis parameter vanishes. A posteriori, not paying attention to geostrophic balance is justified since the results of the operational systems mentioned above show that data assimilation in equatorial ocean models has a beneficial impact.

Nevertheless, the situation is not ideal. Velocities near the equator are relatively poorly simulated in oceanic circulation models. The reason cannot be inadequate forcing data alone. For example, examining again the data of an identical-twin assimilation experiment that had resulted in much improved density and sea-level estimates (Vossepoel and Behringer 2000), we found that velocities actually were degraded rather than improved by the data assimilation procedure (see Fig. 1).

Our hypothesis is that the poor performance of this type of assimilation for velocities compared to densities is due to the lack of balance in the data assimilation updates. We test this hypothesis in the controlled, much simplified, context of a 1.5-layer shallow-water model that reflects the main baroclinic mode of a general oceanic circulation model. A simple assimilation scheme that nudges model height to observed height is the analogy of an optimal interpolation scheme that assimilates temperature and sea-level observations for improving the density structure. As a possible improvement, an alternative assimilation scheme is considered, where zonal velocity and height increments are related by geostrophic balance. In spite of the vanishing Coriolis parameter at the equator, this can be accomplished at the equator too, under rather general assumptions.

Model and methods are presented in section 2. The results of identical twin experiments with the schemes are reported in section 3. Both schemes have a good performance for height, but the simple scheme has a bad performance for zonal velocity while the alternative scheme has a good performance for zonal velocity. In section 4, a brief discussion is given of a generalization of the alternative scheme to 3D models. First tests in data assimilation experiments with two equatorial ocean general circulation models show a positive impact. The implications of the results are discussed in section 5. This is followed by a conclusion.

2. Model, assimilation procedure, and experimental setup

The studies were performed with a linear shallow-water model for the upper tropical Pacific Ocean. The model can be forced by wind stress terms X and Y that act on the zonal velocity u and the meridional velocity v, and by a heat source Q that acts on the height h (i.e., the thermocline depth). The model equations are

$$\frac{\partial u}{\partial t} - fv + g'\frac{\partial h}{\partial x} + F_M(u) = X \qquad (1)$$

$$\frac{\partial v}{\partial t} + fu + g'\frac{\partial h}{\partial y} + F_M(v) = Y \qquad (2)$$

$$\frac{\partial h}{\partial t} + H\left(\frac{\partial u}{\partial x} + \frac{\partial v}{\partial y}\right) + F_H(h) = Q, \qquad (3)$$

with $f = \beta y$ the Coriolis parameter in the beta-plane approximation, and g' reduced gravity; $F_M(u)$, $F_M(v)$, and $F_H(h)$ are frictional terms. The value of the shallow water wave speed $c_0 = (g'H)^{0.5}$ was 2 m s^{-1} in the runs of this paper. More details can be found in the appendix.

Forcing the model with the Florida State University wind stress product (Stricherz et al. 1997) yields a depth anomaly over the Niño-3 region that has a correlation of about 0.8 with the observed Niño-3 temperature index, which is an indication that the model is able to capture the main characteristic of interannual variability in the eastern Pacific.

Assimilation of height observations was done by nudging schemes. Two such schemes have been used. The first is the simple scheme that just nudges model heights h_{fg} to observed heights h_{obs}:

$$h_{ana} = h_{fg} + \alpha(h_{obs} - h_{fg}), \qquad (4)$$

with α a constant, and h_{ana} the height after assimilation. This was done once a day at every grid point, with $\alpha = 0.2$. The quantity $\Delta h = h_{ana} - h_{fg}$ is called the height increment throughout this paper.

The second is the alternative scheme where in addition increments are added to the zonal velocity that are a function of Δh. They are proportional to changes Δu_{geo}, which are in geostrophic balance with the height increments Δh:

$$u_{ana} = u_{fg} + \gamma \Delta u_{geo}(\Delta h). \qquad (5)$$

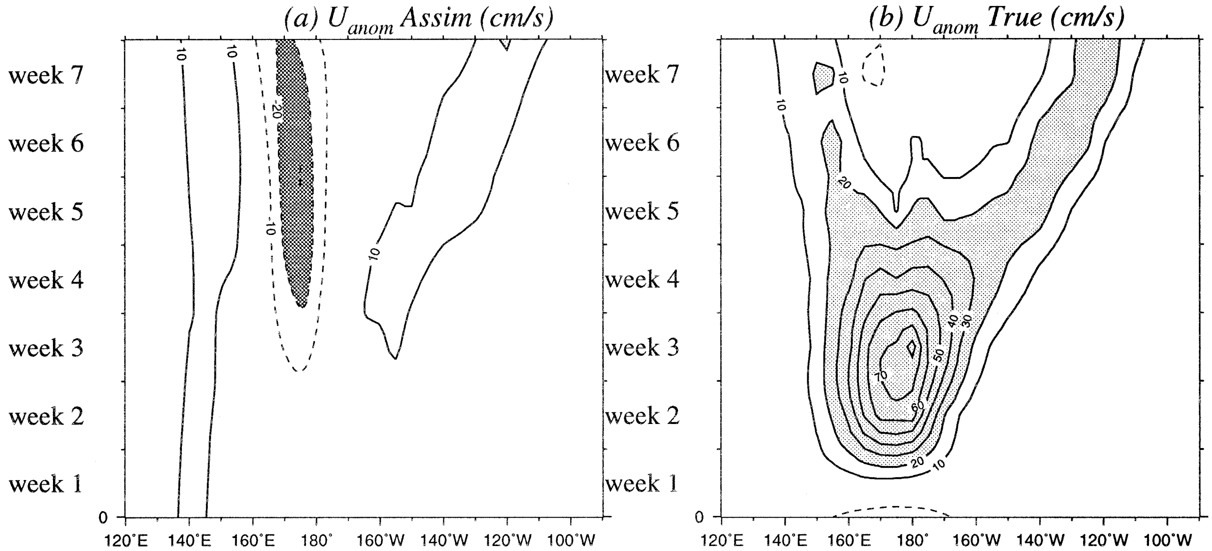

FIG. 1. The effect of temperature assimilation on the zonal velocity field in the NCEP model in an identical twin experiment. Hovmöller diagrams for zonal surface currents for (a) the run with temperature assimilation, (b) the truth run. Shown are differences of zonal surface velocities along the equator with respect to a control run without data assimilation.

We take $\gamma < 1$, because zonal velocity and height model errors are not in exact geostrophic balance. Too high values of γ can even result in numerical instabilities.

Away from the equator, $\Delta u_{\rm geo}(\Delta h)$ is given by

$$\Delta u_{\rm geo}(\Delta h) = -\frac{g'}{f}\frac{\partial \Delta h}{\partial y}. \tag{6}$$

This equation can be used if in (2) one can neglect the meridional velocity terms and the forcing, or rather the errors in these terms. Around the equator, this is a reasonable approximation. For the meridional velocity, no such simple $\upsilon_{\rm geo}$ can be found because neglecting the zonal velocity terms and the forcing in (1) is not a good approximation. At the equator, where (6) cannot be used directly, $u_{\rm geo}$ was estimated by taking the y derivative of $f\Delta u = -g'\partial\Delta h/\partial y$ (Bryden and Brady 1985):

$$\Delta u_{\rm geo}(0°) = -\frac{g'}{\beta}\frac{\partial^2 \Delta h}{\partial y^2}(0°), \tag{7}$$

with $\beta = df/dy(0°)$. The more simple alternative of averaging the values just north and south of the equator, at 1°N and 1°S, gives almost identical results.

The model and assimilation schemes were tested in identical twin experiments. Simulated observations were assimilated into a model run with no forcing. These runs are referred to as assimilation runs. The duration of the runs was 90 days. The observations were generated by forced runs, again by the shallow-water model. These runs are referred to as truth runs. The observations were made nonperfect by averaging over nine grid points in a three-by-three square. Two types of forcing have been considered: zonal wind-patch forcing of the u equation, and heat-patch forcing of the h equation. The patch had a Gaussian dependence on latitude and longitude, with length scales of about 4° and 13° centered on the equator at 170°W. The patch was decaying with a timescale of 10 days and switched off completely after 40 days.

3. Results

Figure 2 shows for the wind-patch truth run time–longitude diagrams on the equator of height and zonal velocity. Time runs upward, up to 90 days. Longitude ranges from 122°E to 68°W. The most pronounced feature is an eastward moving downwelling Kelvin wave. Also, a slower westward propagating upwelling Rossby wave can be seen. In addition there are some wiggles with a preferred timescale of about 6 days, due to inertia–gravity waves. Note that in the height field, the Kelvin and Rossby wave have the opposite sign, while in the zonal velocity field, they have the same sign. This is related to the fact that a wind patch transfers momentum to the ocean, but no heat content.

The result of the simple assimilation scheme at the equator is shown in Fig. 3. The assimilated heights are close to the true heights, which is not surprising given the number of direct height observations. However, the zonal velocity field of the assimilation run is quite different from that of the truth run. In particular, *negative* velocities appear in a region where the truth run has rather pronounced *positive* velocities. As described in section 2, the observations are good but not quite perfect; the assimilation is done once a day, and in (4), $\alpha = 0.2$. The quantity of the observations matters. In the extreme case that the model heights are replaced with the true heights, the zonal velocity errors are typically reduced by a factor of 2 (not shown).

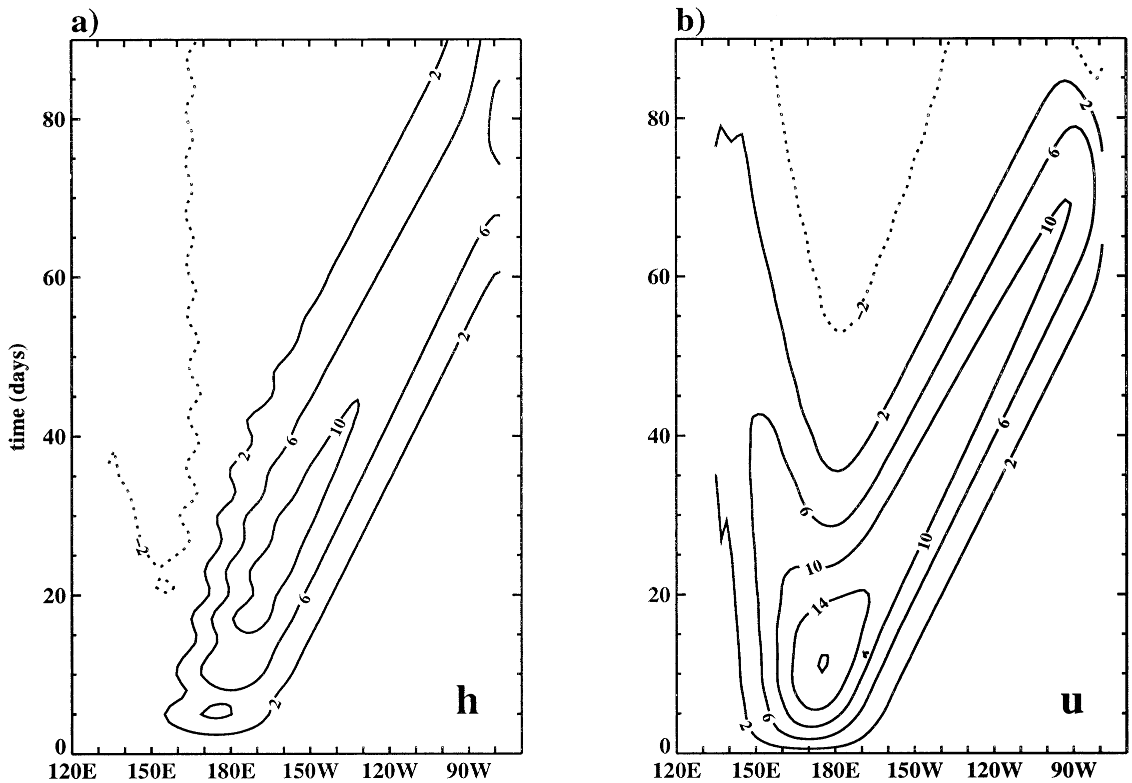

FIG. 2. Hovmöller diagrams for height (a) and zonal velocity (b) for the shallow-water model truth run forced by the wind patch. Time goes upward for 90 days.

The situation at the equator is much better with the alternative scheme that uses zonal velocity increments that are in geostrophic balance with height increments. Figure 4 shows the zonal velocity field, for $\gamma = 0.75$ in (5). The amplitude of the height field is improved too, but at the cost of a slight reduction in the quality of the representation of the wiggles due to gravity waves in the height field contours. For $\gamma = 1$ the zonal velocity field is very similar (not shown), but with stronger low-frequency inertial–gravity waves superimposed.

For a heat patch, the difference between the performance of the two schemes remains small. Figure 5 shows for the heat-patch truth run time–longitude diagrams at the equator of height and zonal velocity. In this case, in the height field, the Kelvin and Rossby wave have the same sign while, in the zonal velocity field, they have the opposite sign. This is related to the fact that a heat patch transfers heat content to the ocean, but no momentum. Note that the Kelvin wave part of the response of the heat patch is very similar to that of the wind patch. Figures 6 and 7 show for this case the results of the simple assimilation scheme and the alternative scheme. Both schemes are able to reproduce both height and zonal velocity fields well.

Off the equator, there is no pronounced difference between the zonal velocity analyses of the two schemes.

4. Implementation in ocean general circulation models

We have implemented the approach outlined above as extensions of existing optimal interpolation schemes and made tests with two ocean general circulation models. In our setup, the changes in density that result from the temperature assimilation are used to compute the effect on dynamic height at every model level. The zonal velocity changes are calculated from the effect on dynamic height. Note that density changes at a certain level affect the dynamic height and velocity at all higher levels, but not at lower levels. There is no change in velocity below the lowest level with density changes, and the change in surface velocity follows directly from the change in sea level.

First, we tested whether the balanced assimilation scheme could improve on the velocities shown in Fig. 1 of the identical twin experiment of Vossepoel and Behringer (2000), who used the ocean model of the seasonal forecasting system of the National Centers for Environmental Prediction (NCEP). The zonal velocity increments were added in the same way as the temperature increments, that is, at three consecutive 1-h time steps every eight time steps. In (5), $\gamma = 0.9$ was used. The result is shown in Fig. 8. Comparing to Fig. 1, one

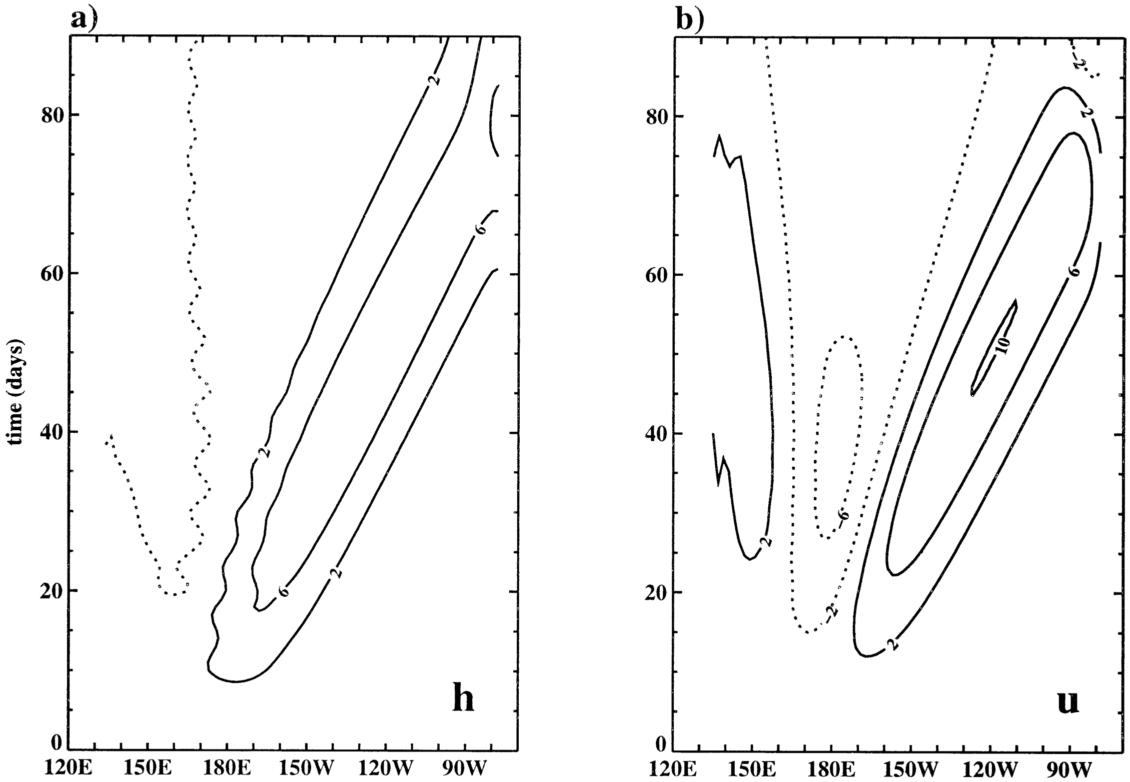

FIG. 3. As in Fig. 2 but for the run where the simple assimilation scheme is used for assimilating height observations from the wind-patch truth run.

can see that the surface velocities are markedly improved with respect to the original scheme.

Next we have performed a test of the scheme in a real ocean data assimilation context, in the system used at European Centre for Medium-Range Weather Forecasts to initialize seasonal forecasts (Stockdale et al. 1998), which uses the Hamburg Ocean Primitive Equation (HOPE) ocean model. In the original scheme, subsurface temperature measurements are used for correcting temperature. The increments are not applied at once, but spread over 10 days, to avoid the generation of gravity waves. In the new scheme, also zonal velocity increments are added as in (5). For the results below we have used $\gamma = 1$.

In the original scheme, the assimilation stops the model temperature from drifting away from climatology, but at the price of a relatively unrealistic zonal velocity at the equator; see the section along the equator in Fig. 9. There is no westward surface current in the east, and between 160° and 110°W there is little shoaling of the equatorial undercurrent from the east to the west, in contrast to observations (Johnson et al. 2001; Yu and McPhaden 1999). In the new scheme, with the geostrophic zonal velocity increments added, the representation of zonal velocity is improved considerably, see Fig. 10, without degradation of the temperature field (not shown).

5. Discussion

At the equator for wind-forced situations, the simple assimilation scheme for the shallow-water model that uses height information for only updating the model height field can lead to a degradation of the zonal velocity field. This is not the case for the alternative assimilation scheme that has zonal velocity increments that are related by geostrophic balance to the height increments. Off the equator, the problem does not arise. Clearly, the problem does not show up in filtered models. An example is the ocean component of the Cane–Zebiak model (Zebiak and Cane 1987) where the long-wave approximation (Philander 1990) ensures that the zonal current is in geostrophic balance with the height field.

In shallow-water models and more complicated models, density information alone is not sufficient to specify the system completely. However, one can use the fact that the system tends to a state that is close to geostrophic balance. From potential vorticity conservation it follows (Daley 1991) that for scales large compared to the Rossby radius, the heights of the adjusted state are less affected than the rotation of the velocities, while for the small scales it is the other way round. So assimilation schemes that assimilate density information only give reasonable estimates for the velocities for the large

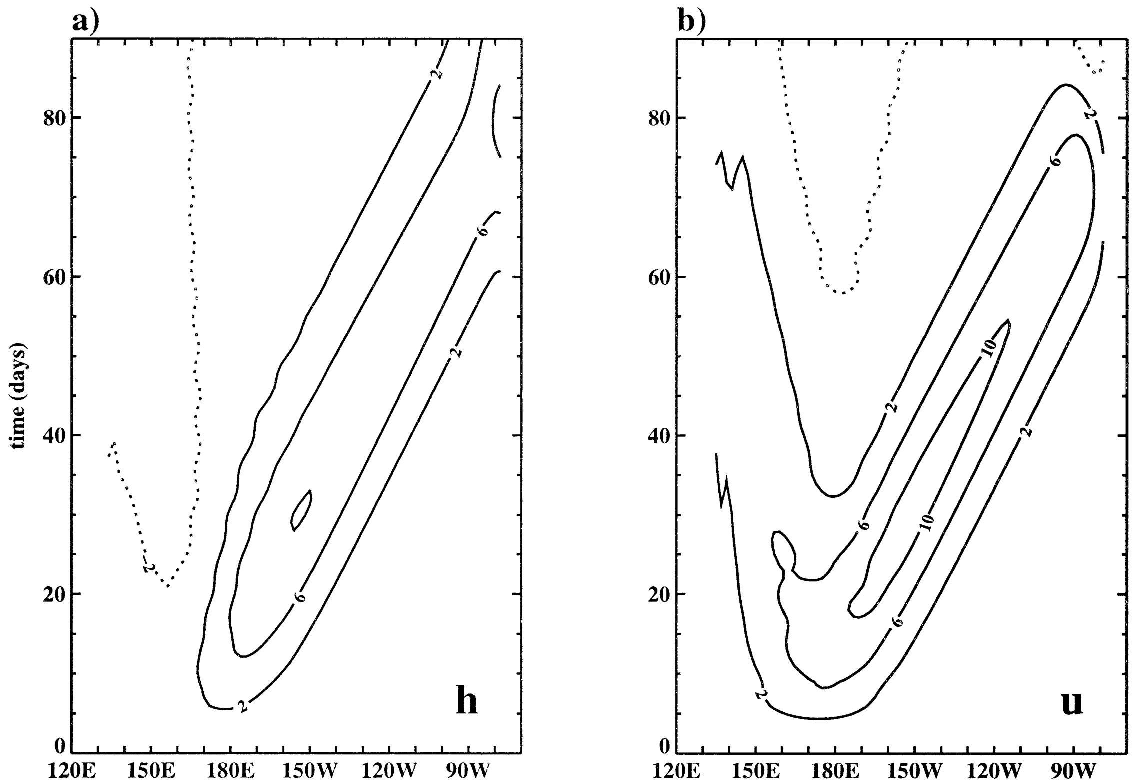

FIG. 4. As in Fig. 2 but for the run where the balanced assimilation scheme is used for assimilating height observations from the wind-patch truth run.

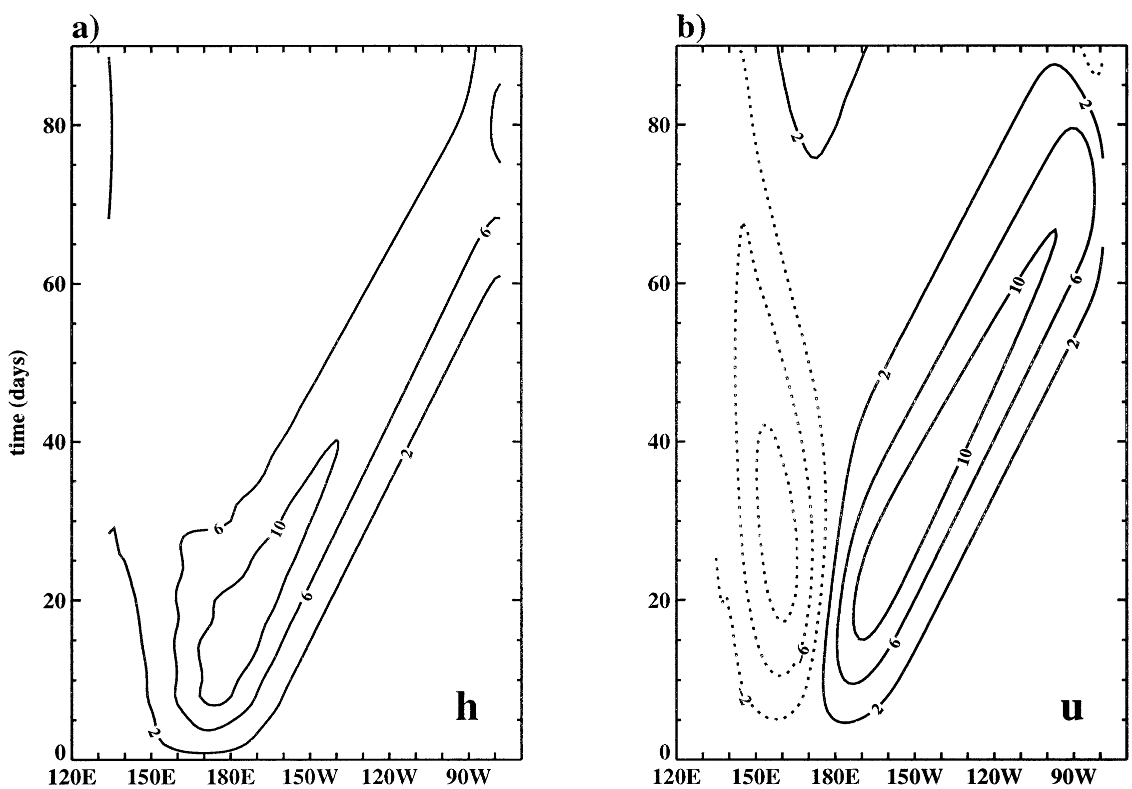

FIG. 5. As in Fig. 2 but for the shallow-water model truth run forced by the heat patch.

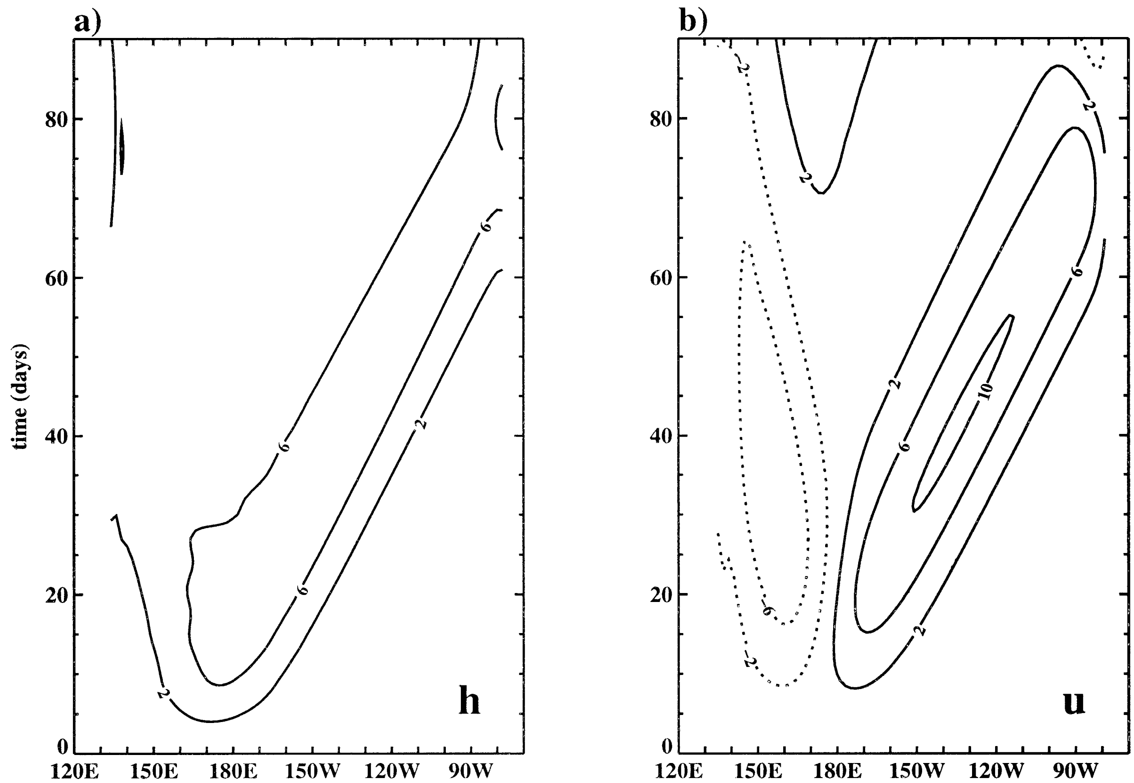

FIG. 6. As in Fig. 2 but for the run where the simple assimilation scheme is used for assimilating height observations from the heat-patch truth run.

scales, while the small scales are inherently problematic. Fortunately, in the ocean the Rossby radius is small compared to the scale of continents and ocean basins. So for many applications, density information can be sufficient for an adequate estimate of the ocean state. Close to the equator, where the Rossby radius is relatively large and the separation between the timescales of planetary waves and inertial–gravity waves is relatively small, this may require some extra care.

One can view a nudging or an OI type of scheme as a scheme where extra forcings are added in order to get the ocean state closer to the observations. In case only density is affected, only heat and possibly salt sources are added, while the mismatch between the ocean state and the observations is also due to errors in the wind forcing. This leads to the question of how well heat forcing can mimic the effect of wind forcing, a problem addressed, for example, in the textbook of Gill (1982). If the forcing (X, Y, Q) in (1)–(3) gives rise to the fields (u, v, h), then there exists a forcing $(0, 0, Q + w_E)$ that gives rise to the fields $(u + u_E, v + v_E, h)$. In other words, there exists a forcing of the heat equation only that yields the same height field. The difference in the velocities, u_E and v_E, satisfies the Ekman equations and is local in space, and approximately local in time (timescale f^{-1} off the equator). The magnitude of the difference scales with f^{-1}, and for a typical wind stress and layer depth has a value of 25 cm s^{-1} at 2°N compared to 1 cm s^{-1} at 45°N. Closer to the equator, scaling with f^{-1} breaks down because friction starts to play a role. This explanation also applies when comparing the two data assimilation schemes, where the two different external forcings give in first approximation the same height fields. So the difference in the velocity between the schemes is expected to scale with f^{-1} as well. Note that although the effect is local in time, if the data assimilation is to correct a model bias, this will result in a difference at all times between the schemes.

The difference between the zonal velocities in the assimilation schemes arises through gravity waves. This can be seen in latitude–longitude pictures (not shown). If only the height is corrected in the data assimilation procedure, attempting to reproduce the effect of the wind forcing by a heat forcing, then the change in pressure gradient does not correspond to a change in wind forcing, and the change in pressure gradient will cause velocity tendencies, see (1) and (2), and create spurious gravity waves. In the truth run, wind forcing causes zonal velocity changes and zonal velocity leads height. In the assimilation run, however, height leads zonal velocity, and the added water simply flows away in all directions during the days before equatorial adjustment sets in. Moreover, adjustment is not to the truth state, and around the equator the small differences lead to a geostrophic velocity that has the wrong sign in the windpatch region compared to the truth run. Additional tests

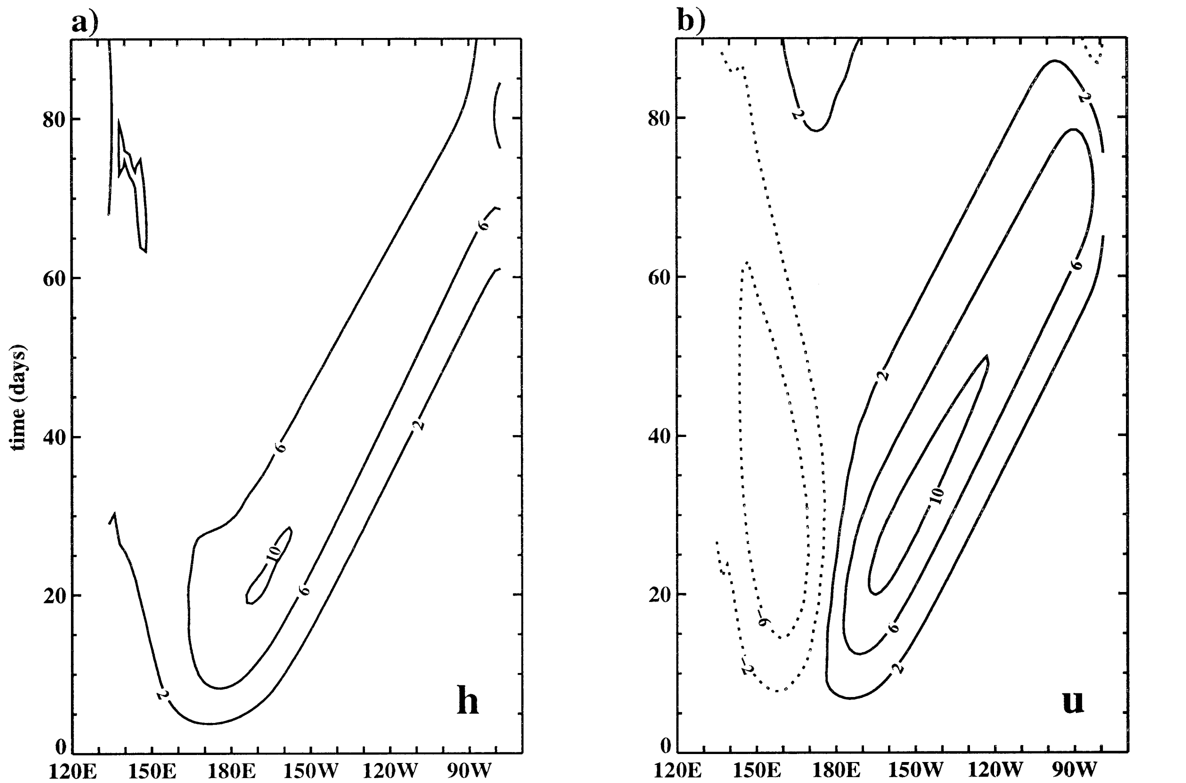

FIG. 7. As in Fig. 2 but for the run where the balanced assimilation scheme is used for assimilating height observations from the heat-patch truth run.

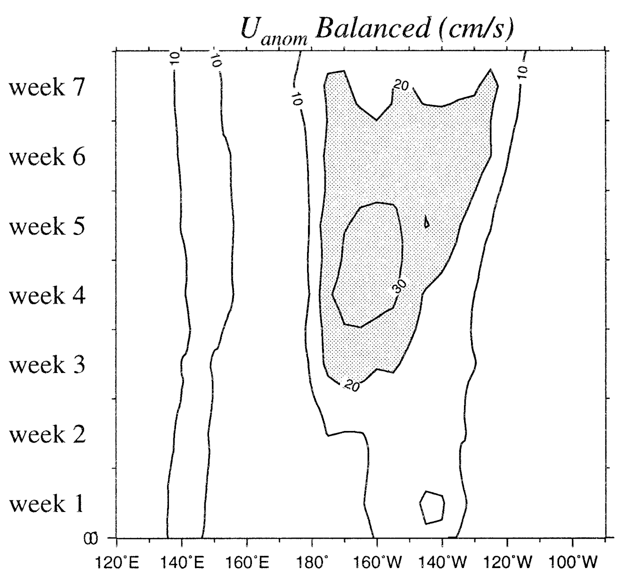

FIG. 8. The effect of balanced assimilation of temperatures on the surface zonal velocity field in the NCEP model in an identical twin experiment. Hovmöller diagrams for zonal surface currents for the run with the balanced assimilation scheme, instead of the scheme used in Fig. 1a.

with the shallow-water model show that this even occurs if the height increment is spread out in time and the amplitude of the gravity waves reduced. Nonperfect observations make this even worse. In a run with balanced increments, the increments cause no gravity waves directly, as gravity waves are not in zonal geostrophic balance.

A complication is that zonal velocity and height errors are not in exact geostrophic balance. An extreme case is when perfect height observations are assimilated in the absence of forcing. Clearly, the assumption that height and zonal velocity errors are in geostrophic balance does not apply here. Also, the homogeneous part of the equations is subtly changed by (5)–(6) in a way that preferentially damps components that are in zonal geostrophic balance, as the system wishes to replace this component by observations. Thus inertial–gravity waves may be damped less than in the system with no data assimilation, or may even grow (e.g., for $\alpha = 0.3$, $\gamma = 1$). To remedy this situation, the zonal velocity increments are multiplied with a factor γ, see (5). A rule of thumb is that one should have $\gamma < 1$, to account for the part of the error not in zonal geostrophic balance, and that the damping time of long waves should be longer than the Rossby period $[2\pi(\beta c)^{-0.5}]$, in order to make geostrophic adjustment of the flow possible.

One might wonder whether very close to the equator

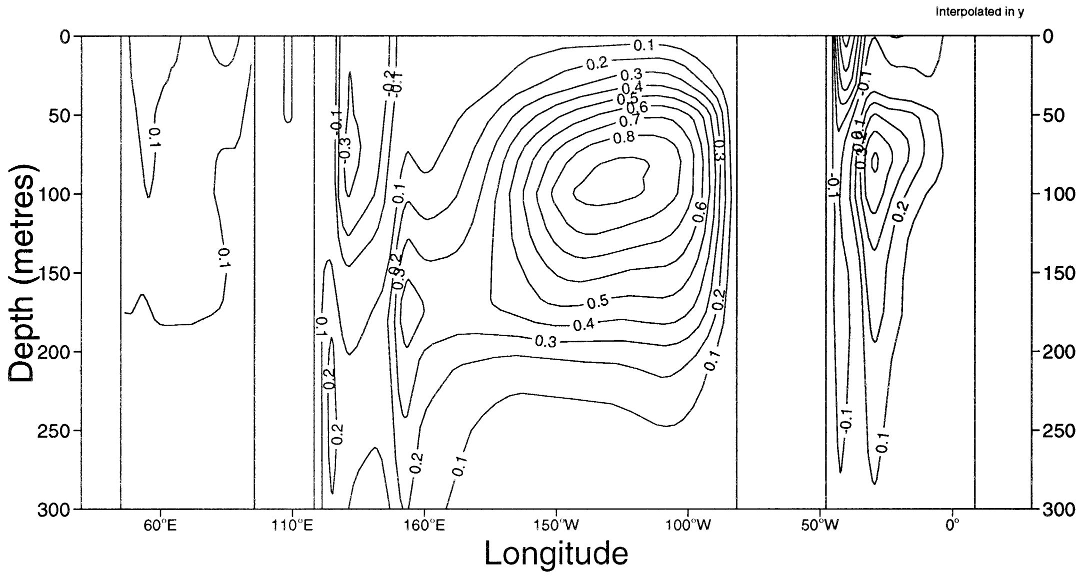

FIG. 9. Mean zonal velocity (m s^{-1}) in a section along the equator of a HOPE model run with a subsurface temperature assimilation scheme that has temperature, but no zonal velocity increments.

geostrophic balance does not pose a problem since (6) does not have a well-defined limit at the equator. However, one should keep in mind that derivatives should always be evaluated at an appropriate scale. In the case at hand, an appropriate scale near the equator is a considerable fraction of the equatorial Rossby radius. At the equator, this leads to (7), where the second derivative should be evaluated at the same scale as used in (6).

The approach outlined above has been generalized to two optimal interpolation schemes for general circulation models. First, in the identical twin experiment with the NCEP model, the gross error in the surface velocity of the original scheme was eliminated. Second, in the real data assimilation experiment using the HOPE model, the mean current in the eastern Pacific was improved, especially in the surface layer. More tests will be necessary to determine whether currents are systematically improved or not with the present generalization of the balanced data assimilation scheme, and how to determine the optimal choice for the factor γ in (5). Perhaps a more sophisticated multivariate OI scheme would perform significantly better than the present, more naive,

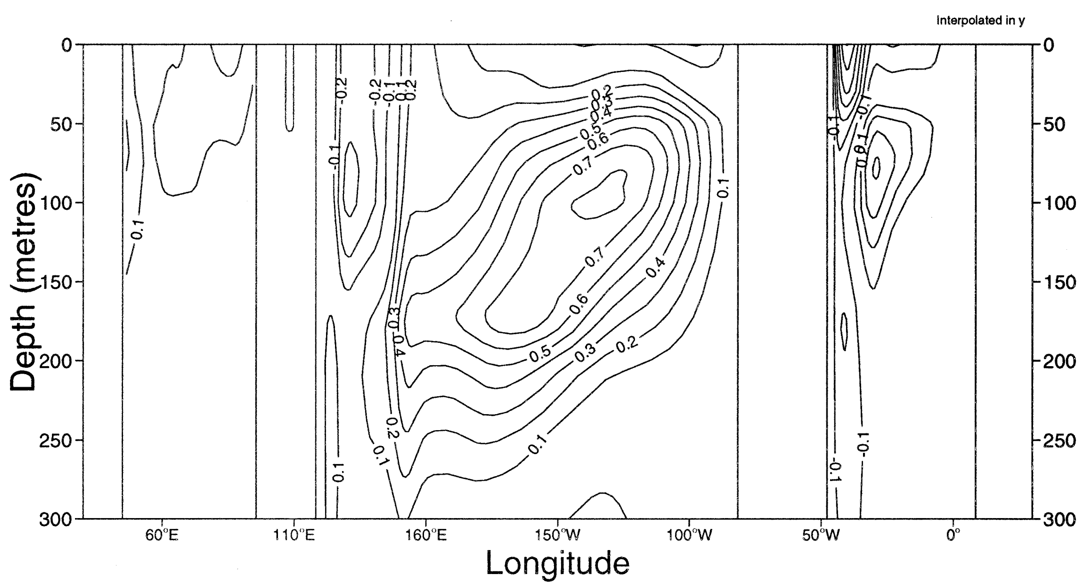

FIG. 10. Mean zonal velocity (m s^{-1}) in a section along the equator of a HOPE model with a subsurface temperature assimilation scheme that has both temperature and zonal velocity increments.

implementation. These questions, and the impact of the scheme on the forecasts, still need to be addressed.

In more advanced data assimilation methods, such as Kalman filtering and 4D-VAR schemes, the need for balanced updates has consequences for the proper formulation of background error covariance matrices. The control variables may already implicitly contain the geostrophic balance [e.g., the wind updates in Bonekamp et al. (2001)]. If they do not, the balance must be ensured by a multivariate error covariance matrix that makes nongeostrophic updates unlikely.

Note, however, that using more advanced data assimilation methods can never compensate for an intrinsic lack of information about the currents. So if the forcing errors cannot be neglected and the small-scale velocity structures should be estimated as well, it is not sufficient to have density information only, irrespective of the assimilation method used.

6. Conclusions

Assimilation schemes of the type that is used for seasonal forecasts can have a problem in estimating zonal velocities. This is the case for OI schemes that use density information for updating only the model density field, which in some situations leads to a detoriation of the zonal velocity field around the equator. A possible remedy has been tested and cures the problem in a simple linear shallow-water model. It updates the zonal velocity with increments that are related to the density increments by geostrophic balance. A straightforward generalization of the method has been implemented in two ocean circulation models, and first tests show a positive impact on surface currents.

Acknowledgments. Helpful discussions with David Anderson, Gerbrand Komen, and Jerome Vialard are gratefully acknowledged. We thank Ming Ji, Dick Reynolds, and Dave Behringer for making available and explaining the NCEP model and analysis system. Computing resources for the computations with NCEP model were provided by the Center for High Performance applied Computing (HPαC) of Delft University of Technology. PJVL was supported by the National Research Program, Grant 013001237.10.

APPENDIX

Linear Shallow-Water Model

The shallow-water model of the tropical Pacific is a 1.5-layer linear model of a baroclinic mode on a beta plane. It describes the thermocline depth field h, the zonal velocity field u, and the meridional velocity v of a shallow water layer of mean thickness H and density ρ over a motionless bottom layer of density $\rho + \Delta\rho$. The model can be forced by wind stress terms X and Y that act on u and v, and by a heat source Q that acts on h. The model equations are

$$\frac{\partial u}{\partial t} - \beta y v + g'\frac{\partial h}{\partial x} + F_M(u) = X \qquad \text{(A1)}$$

$$\frac{\partial v}{\partial t} + \beta y u + g'\frac{\partial h}{\partial y} + F_M(v) = Y \qquad \text{(A2)}$$

$$\frac{\partial h}{\partial t} + H\left(\frac{\partial u}{\partial x} + \frac{\partial v}{\partial y}\right) + F_H(h) = Q, \qquad \text{(A3)}$$

where, as usual, x denotes longitude and y latitude. For the Coriolis parameter f the beta-plane approximation $f = \beta y$ is used, $g' = g\rho^{-1}\Delta\rho$ is the reduced gravity; $F_M(u)$, $F_M(v)$, and $F_H(h)$ are linear frictional terms. The value of the shallow water wave speed $c_0 = (g'H)^{0.5}$ was 2 m s^{-1} in the runs of this paper, and the mean depth H was set to 150 m.

The frictional terms consist of several parts. The main part is the harmonic part, with an eddy viscosity of 2×10^4 m^2 s^{-2} in F_M and an eddy diffusivity of 2×10^3 m^2 s^{-2} in F_H. A linear damping term, which is only sizable near the northern and southern boundary of the basin, prevents waves propagating along these boundaries. Small terms proportional to the fourth derivative in the x and y directions are used to damp short-wave length instabilities near the equator. The coefficients of the fourth-order terms are of the order of 0.01, when made dimensionless with the model time step and model grid spacing.

The model equations (A1)–(A3) are implemented on a C grid in a standard way, see, for example, the textbook of Kantha and Clayson (2000), over a closed basin. The western boundary and eastern boundary follow approximately the coastlines of Australasia and America, and the southern and northern boundary are at 30°S and 30°N. The standard grid spacing is 2° in the zonal direction, and 1° in the meridional direction. With this resolution, the main limit on the time step comes from the explicit treatment of the Coriolis terms near the northern and southern boundaries. The standard time step is 8 h.

The time stepping scheme of the model is as follows. At each step, new values (h_1, u_1, v_1) are obtained from the old values (h_0, u_0, v_0) as follows:

$$\begin{aligned} h_1 &= h_1(h_0, u_0, v_0) \\ u_1 &= u_1(h_1, u_0, v_0) \\ v_1 &= v_1(h_1, u_1, v_0). \end{aligned} \qquad \text{(A4)}$$

This scheme allows for a relatively large time step with little need for storage compared to more standard schemes where u and v are evaluated at the same time level. In the assimilation runs, the increments are calculated and added right after the calculation of a new height field.

A test to study the influence of the resolution has been performed with a grid spacing of 0.5° lat by 1° lon and a time step of 6 h for the wind patch run of section 3. Not only are the Kelvin and Rossby waves the same, also the wiggles of the inertial–gravity waves showed no difference. In fact, there was hardly any discernible difference between the standard and the high resolution run.

REFERENCES

Alves, J. O. S., K. Haines, and D. L. T. Anderson, 2001: Sea level assimilation experiments in the tropical Pacific. *J. Phys. Oceanogr.,* **31,** 305–323.

Behringer, D. W., M. Ji, and A. Leetmaa, 1998: An improved coupled model for ENSO prediction and implications for ocean initialization. Part I: The ocean data assimilation system. *Mon. Wea. Rev.,* **126,** 1013–1021.

Bell, M. J., M. J. Martin, and N. K. Nichols, 2001: Assimilation of data into an ocean model with systematic errors near the equator. Hadley Centre for Climate Prediction and Research, Met Office, Ocean Applications Tech. Note 27, Bracknell, United Kingdom, 27 pp.

Bonekamp, H., G. J. van Oldenborgh, and G. Burgers, 2001: Variational assimilation of Tropical Atmosphere–Ocean and expendable bathythermograph data in the Hamburg Ocean Primitive Equation ocean general circulation model, adjusting the surface fluxes in the tropical ocean. *J. Geophys. Res.,* **106,** 16 693–16 709.

Bryden, H. L., and E. C. Brady, 1985: Diagnostic model of the three-dimensional circulation in the upper equatorial Pacific Ocean. *J. Phys. Oceanogr.,* **15,** 1255–1261.

Daley, R., 1991: *Atmospheric Data Analysis.* Cambridge University Press, 457 pp.

Gill, A., 1982: *Atmosphere–Ocean Dynamics.* Academic Press, 662 pp.

Ishikawa, Y., T. Awaji, and N. Komori, 2001: Dynamical initialization for the numerical forecasting of ocean surface circulations using a variational assimilation scheme. *J. Phys. Oceanogr.,* **31,** 75–93.

Ji, M., A. Leetmaa, and V. E. Kousky, 1996: Coupled model predictions of ENSO during the 1980s and 1990s at the National Centers for Environmental Prediction. *J. Climate,* **9,** 3105–3120.

——, R. W. Reynolds, and D. W. Behringer, 2000: Use of TOPEX/Poseidon sea level data for ocean analyses and ENSO prediction: Some early results. *J. Climate,* **13,** 216–231.

Johnson, G. C., M. J. McPhaden, and E. Firing, 2001: Equatorial Pacific Ocean horizontal velocity, divergence, and upwelling. *J. Phys. Oceanogr.,* **31,** 839–849.

Kantha, L. H., and C. A. Clayson, 2000: *Numerical Models of Oceans and Oceanic Processes.* Academic Press, 936 pp.

Oschlies, A., and J. Willebrand, 1996: Assimilation of Geosat altimeter data into an eddy-resolving primitive equation model of the North Atlantic Ocean. *J. Geophys. Res.,* **101,** 14 175–14 190.

Philander, S. G. H., 1990: *El-Niño, La Niña, and the Southern Oscillation.* Academic Press, 291 pp.

Segschneider, J., D. L. T. Anderson, and T. N. Stockdale, 2000: Toward the use of altimetry for operational seasonal forecasting. *J. Climate,* **13,** 3115–3138.

Smith, N., J. E. Blomley, and G. Meyers, 1991: A univariate statistical interpolation scheme for subsurface thermal analyses in the tropical oceans. *Progress in Oceanography,* Vol. 28, Pergamon, 219–256.

Stockdale, T. N., D. L. T. Anderson, J. O. S. Alves, and M. A. Balmaseda, 1998: Global seasonal rainfall forecasts using a coupled ocean–atmosphere model. *Nature,* **392,** 370–373.

Stricherz, J., D. Legler, and J. O'Brien, 1997: *TOGA Pseudo-stress Atlas 1985–1994. Vol. II, Pacific Ocean.* Florida State University, 158 pp.

Vossepoel, F. C., and D. W. Behringer, 2000: Impact of sea level assimilation on salinity variability in the western equatorial Pacific. *J. Phys. Oceanogr.,* **30,** 1706–1721.

Yu, X., and M. J. McPhaden, 1999: Seasonal variability in the equatorial Pacific. *J. Phys. Oceanogr.,* **29,** 925–947.

Zebiak, S. E., and M. A. Cane, 1987: A model El Niño–Southern Oscillation. *Mon. Wea. Rev.,* **115,** 2262–2278.